AMERICAN SOCIETY FOR MICROBIOLOGY | Antimicrobial Agents and Chemotherapy®

MECHANISMS OF ACTION: PHYSIOLOGICAL EFFECTS

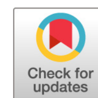

Search for a Shared Genetic or Biochemical Basis for Biofilm Tolerance to Antibiotics across Bacterial Species

Philip S. Stewart,[a,b] Kerry S. Williamson,[a,c] Laura Boegli,[a] Timothy Hamerly,[a,d] Ben White,[a,c] Liam Scott,[a,d] Xiao Hu,[e] Brendan M. Mumey,[e] Michael J. Franklin,[a,c] Brian Bothner,[a,d] Francisco G. Vital-Lopez,[f,g] Anders Wallqvist,[f] Garth A. James[a]

[a]Center for Biofilm Engineering, Montana State University, Bozeman, Montana, USA
[b]Department of Chemical and Biological Engineering, Montana State University, Bozeman, Montana, USA
[c]Department of Microbiology and Cell Biology, Montana State University, Bozeman, Montana, USA
[d]Department of Chemistry and Biochemistry, Montana State University, Bozeman, Montana, USA
[e]Gianforte School of Computing, Montana State University, Bozeman, Montana, USA
[f]Department of Defense Biotechnology High Performance Computing Software Applications Institute, Telemedicine and Advanced Technology Research Center, U.S. Army Medical Research and Development Command, Fort Detrick, Maryland, USA
[g]The Henry M. Jackson Foundation for the Advancement of Military Medicine, Inc., Bethesda, Maryland, USA

ABSTRACT Is there a universal genetically programmed defense providing tolerance to antibiotics when bacteria grow as biofilms? A comparison between biofilms of three different bacterial species by transcriptomic and metabolomic approaches uncovered no evidence of one. Single-species biofilms of three bacterial species (*Pseudomonas aeruginosa*, *Staphylococcus aureus*, and *Acinetobacter baumannii*) were grown *in vitro* for 3 days and then challenged with respective antibiotics (ciprofloxacin, daptomycin, and tigecycline) for an additional 24 h. All three microorganisms displayed reduced susceptibility in biofilms compared to planktonic cultures. Global transcriptomic profiling of gene expression comparing biofilm to planktonic and antibiotic-treated biofilm to untreated biofilm was performed. Extracellular metabolites were measured to characterize the utilization of carbon sources between biofilms, treated biofilms, and planktonic cells. While all three bacteria exhibited a species-specific signature of stationary phase, no conserved gene, gene set, or common functional pathway could be identified that changed consistently across the three microorganisms. Across the three species, glucose consumption was increased in biofilms compared to planktonic cells, and alanine and aspartic acid utilization were decreased in biofilms compared to planktonic cells. The reasons for these changes were not readily apparent in the transcriptomes. No common shift in the utilization pattern of carbon sources was discerned when comparing untreated to antibiotic-exposed biofilms. Overall, our measurements do not support the existence of a common genetic or biochemical basis for biofilm tolerance against antibiotics. Rather, there are likely myriad genes, proteins, and metabolic pathways that influence the physiological state of individual microorganisms in biofilms and contribute to antibiotic tolerance.

KEYWORDS antibiotic, biofilms, metabolomic, physiology, tolerance, transcriptomic

Because antimicrobial tolerance appears to be a universal, ancient, and ubiquitous phenotype associated with biofilm formation (1–5), it is logical to postulate the existence of a conserved genetic or biochemical basis for the biofilm defense against antibiotics. Hypothesizing the existence of this defense, we made these predictions: (i) a set of conserved genes is differentially expressed in biofilms compared to planktonic genes (and a subset of these genes can be associated with antibiotic tolerance), (ii) common genetically encoded functions are differentially expressed in biofilms compared to planktonic cells (and some of these shared functions can be associated with antibiotic tolerance), (iii) a set of conserved genes is differentially expressed in biofilms in response to antibiotic treatment (and a

Copyright © 2022 American Society for Microbiology. All Rights Reserved.
Address correspondence to Philip S. Stewart, phil_s@montana.edu.
The authors declare no conflict of interest.
Received 7 January 2022
Returned for modification 23 January 2022
Accepted 29 January 2022
Published 10 March 2022

Downloaded from https://journals.asm.org/journal/aac on 19 April 2022 by 153.90.118.208.

TABLE 1 Antibiotic efficacy against planktonic and biofilm bacteria[a]

Organism	Antibiotic	Concn (μg mL^{-1})	X_o, log$_{10}$ (CFU cm^{-2})	LR$_P$	LR$_B$	TF
P. aeruginosa	CIP	1	9.18 ± 0.26	4.46	1.79 ± 0.43	2.5
A. baumannii	TIG	20	8.95 ± 0.15	3.32	0.92 ± 0.06	3.6
S. aureus	DAP	10	9.35 ± 0.17	2.35 ± 0.29	1.37 ± 0.18	1.7

[a]TF denotes the tolerance factor as defined in reference 2, which in this case is the log reduction against planktonic cells divided by the log reduction against biofilm (LR_P/LR_B). X_o denotes viable cell areal density of the untreated control biofilm. CIP, ciprofloxacin; TIG, tigecycline; DAP, daptomycin. Uncertainties are indicated with standard deviations.

subset of these genes can be associated with antibiotic tolerance), (iv) common genetically encoded functions are differentially expressed in antibiotic-treated biofilms compared to untreated biofilms (and some of these shared functions can be associated with antibiotic tolerance), (v) a common pattern of altered metabolism occurs in biofilm compared to planktonic cells (and at least a part of this metabolic shift can be associated with antibiotic tolerance), and (vi) a common pattern of altered metabolism occurs in antibiotic-treated biofilms compared to untreated biofilms (and at least a part of this metabolic shift can be associated with antibiotic tolerance). We undertook to test whether these predictions hold across microbial species and antibiotic types by challenging biofilms formed by three different bacteria with distinct antibiotics clinically appropriate for each organism.

RESULTS

Characterization of the biofilm response to antibiotic treatment. Comparing antibiotic killing of the three bacteria between planktonic and biofilm modes of growth demonstrated consistent reduced susceptibility of cells in biofilms (Table 1). The antibiotics used were ciprofloxacin for *Pseudomonas aeruginosa*, tigecycline for *Acinetobacter baumannii*, and daptomycin for *Staphylococcus aureus*. Within a given bacterial species, the drug concentration and duration of antibiotic exposure (24 h) was the same for planktonic and biofilm challenges. All three untreated control biofilms contained approximately 10^9 CFU cm^{-2}. The biofilm tolerance factor (2) ranged from 1.7 to 3.6 (Table 1). These results confirm that the drip-flow reactor biofilm model captured the commonly observed phenotype of antibiotic tolerance in the biofilm state for all three model organisms: *P. aeruginosa* (5–27), *A. baumannii* (28–34), and *S. aureus* (35–43).

Biofilm compositions for each of the three bacterial species investigated are summarized in Table 2. These measurements were made on the entire biofilm, i.e., cells and extracellular polymeric substances together. In all cases, protein was the most abundant constituent, carbohydrate was intermediate, and DNA was the least abundant constituent. Antibiotic treatment of biofilms resulted in decreases in each of the three biomass constituents for all three species. Averaging across the three species, antibiotic-treated biofilm contained 49% of the protein, 63% of the carbohydrate, and 63% of the DNA compared to their respective untreated control biofilms.

Genes differentially expressed between biofilm and planktonic cells. A global transcriptomic analysis was performed to identify genes that were differentially expressed between 96-h-old drip-flow biofilms and planktonic cells (Table 3). Within each species, transcripts significantly changing at least 2-fold at a P value of <0.05 were selected for use in this analysis. Some of the genes that changed between these two growth conditions could be associated with reduced antibiotic susceptibility. We sought to discover any genes

TABLE 2 Biofilm composition[a]

Condition	Protein (μg cm^{-2})	Carbohydrate (μg cm^{-2})	DNA (μg cm^{-2})
P. aeruginosa, untreated	362 ± 141	184 ± 20	13.9 ± 1.5
P. aeruginosa, CIP treated	83 ± 37	109 ± 16	10.7 ± 2.5
A. baumannii, untreated	134 ± 49	30 ± 10	5.1 ± 1.9
A. baumannii, TIG treated	83 ± 25	24 ± 9	3.5 ± 1.0
S. aureus, untreated	119 ± 32	54 ± 15	7.1 ± 2.2
S. aureus, DAP treated	73 ± 52	27 ± 20	3.0 ± 1.5

[a]Values are given as the means ± standard deviations. CIP, ciprofloxacin; TIG, tigecycline; DAP, daptomycin.

Downloaded from https://journals.asm.org/journal/aac on 19 April 2022 by 153.90.118.208.

TABLE 3 Changes in gene expression between biofilm and planktonic and antibiotic-treated biofilm and untreated biofilm systems[a]

Organism	B:P, up in B	B:P, down in B	TB:B, up in TB	TB:B, down in TB
P. aeruginosa	449	623	255	337
A. baumannii	259	157	692	492
S. aureus	232	321	59	29

[a]Values are the number of genes that changed in the indicated direction by a fold change of 2.0 or greater at $P < 0.05$. B, biofilm; P, planktonic; TB, antibiotic-treated biofilm.

that changed consistently across the three organisms. We acknowledge at the outset that our transcriptomic data are not spatially resolved. Microscale variation in gene expression is known to be common in biofilm systems (16, 38, 44, 45).

We first searched for homology between the three species by inferring orthogroups of protein-coding genes. Protein sequences from *P. aeruginosa* PAO1, *S. aureus* USA300 FPR3757, and *A. baumannii* AB5075 were analyzed using OrthoFinder (46) to identify orthologous groups containing all genes that descended from a single gene in the last common ancestor of the three species. OrthoFinder is advantageous in that it automatically removes gene length bias and phylogenetic distance from sequence similarity scores, making it one of the most accurate and robust orthology inference methods available (47). It was found to be the most accurate method on the Quest for Orthologs benchmark test (48, 49) and was also more accurate than curated online database methods (47). The accuracy of its key component algorithms has been independently assessed and validated (47), making it an appropriate choice for providing a framework for extrapolation between the three species in our study.

A summary of the OrthoFinder results can be found in Table S1 in the supplemental material. By definition, the orthogroups contain both orthologs and paralogs. Of the 2,535 orthogroups identified by the analysis, 30% (763 groups) contained proteins from all three species; 51% (1,283 groups) contained proteins from two of the species, with the greatest number of groups from overlap of the two Gram-negative organisms, *P. aeruginosa* and *A. baumannii*. The remaining 19% (489 groups) contained proteins from within one species. All orthologous groups (81%, or 2,046 groups) that had homology across two or three species were used for analysis in this study.

To further validate this approach, we compared the orthologous groups to results from Xavier et al. (50). Xavier et al. used genome-scale metabolic modeling and data from published large-scale essentiality assays from prokaryotic organisms to identify 28 highly conserved cofactor biosynthesis genes (Table S2). Significant homologs for these genes were found in greater than 86% of the 79 genomes in their modeling study. While two of the species in our study were not investigated by Xavier et al. (only *P. aeruginosa* PAO1 was included in their analysis), we would expect to find homology of these genes in our study as well if the genes are in fact highly conserved and our approach is valid. Of the 28 conserved cofactor biosynthesis genes identified by Xavier et al., 21 were found to be conserved across the three species in our study, and an additional two were conserved in two of the species, bringing the total percentage of biosynthesis genes with some conservation in our study to 86%. To determine if the overlap of orthologous groups found in all three of our species was significant, *P* values were calculated using a negative binomial distribution. Finding 21 of the 28 cofactor biosynthesis genes within the 763 orthologous groups found in all three species in our study does represent significant overlap ($P < 0.00001$), providing evidence that the OrthoFinder analysis is valid.

Using the same approach, Xavier et al. (50) also investigated the conservation of metabolic genes and found transport to be, by far, the most prevalently conserved metabolic subsystem in the prokaryotic organisms analyzed. In particular, ABC transporters had homology across most of the species. To test if transport genes also had homology between the three species in our study, we first identified genes in *Acinetobacter baumannii* whose annotation contained both the text "ABC" and "transport" within the description, and we then evaluated if OrthoFinder identified homologs to these genes within the other two

Downloaded from https://journals.asm.org/journal/aac on 19 April 2022 by 153.90.118.208.

species. *Acinetobacter baumannii* was chosen due to its complete annotation available from multiple sources. Annotation from the array manufacturer MYcroarray (now Arbor Biosciences, Ann Arbor, MI), the Manoil Lab (51), NCBI, and the PATRIC, PFAM, Prosite, and Protein RefSeq databases were examined, and 101 genes were identified from this search. Of the 101 genes annotated to be involved with ABC transport, 33 were found to be present in orthogroups containing all three species ($P < 0.01$), while 52 were found in orthogroups containing two species ($P < 0.001$). Finding significant conservation of transport genes in the orthologous groups in our study provided further support of the validity of our approach.

Since the OrthoFinder program and its identification of homology in *A. baumannii*, *S. aureus*, and *P. aeruginosa* were found to be sound, the resulting orthogroups were used to measure the similarity of these organisms' responses to the biofilm mode of growth to determine if this response was also conserved across the three species. Genes upregulated in biofilms compared to planktonic cultures (Table 3) were evaluated for homologs across the species. For example, of the 232 genes upregulated in *S. aureus* biofilms, 53 were conserved across the three species, while homologs for 10 were found in *P. aeruginosa* and for seven were found in *A. baumannii*. Table S2 summarizes the level of homology for each species and condition of interest, and it serves as a quality control that homology was indeed found and further analysis was appropriate. Next, the orthogroups for the upregulated genes in each species (51 *S. aureus*, 55 *P. aeruginosa*, and 31 *A. baumannii* groups that were found in three species) were searched for a common response across the three species. Only one orthogroup was found to be upregulated in the biofilm mode of growth in all three species, which does not represent a significantly conserved response ($P > 0.99$), as calculated by a hypergeometric distribution. The orthogroup upregulated in biofilms in all three species (OG0000123) contained the ATP-dependent chaperone ClpB as well as the related proteins ClpA and ClpC in *S. aureus*.

After finding no significantly conserved upregulated gene response to the biofilm mode of growth, the genes downregulated in biofilms in the three species were then searched for homology. The genes downregulated in biofilms compared to planktonic cultures were also adequately represented in the OrthoFinder analysis. Of these, four orthogroups were found to contain genes downregulated in all three species (Table S2). This does not represent a significantly similar response in biofilm gene downregulation ($P = 0.93$), as this number would be expected to be found by chance.

Another approach to comparing the differentially expressed genes between the three microbial species is to organize the affected genes into functional groups. This approach is expected to be less stringent than the analysis based on sequence homology. To do this, manually curated lists of genes that changed between biofilm and planktonic conditions were prepared for each microorganism (Table 4). These gene sets were then inspected to identify similar functional groups that changed in the same direction for more than one organism. These common gene sets are highlighted in boldface in Table 4. The only gene set that was common across all three microorganisms was for genes associated with stationary phase.

Mature biofilms are known to exhibit growth limitation, starvation responses, and stationary-phase character (7, 13, 14, 20, 38, 45, 52–59). Working from the literature, we built custom gene lists defining the gene set induced in stationary phase in each of the three microorganisms (60–67) (see the supplemental material). For each bacterium, statistically significant overlap between the stationary-phase gene set and our biofilm-induced gene set was determined (Table 5). This preliminary finding supports the hypothesis that all three biofilms experience restriction of growth and express some stationary-phase character. The gene sets for each of the three microorganisms, however, display little specific or functional overlap (68).

It is interesting that biofilms of all three species, grown in the drip-flow reactor on artificial chronic wound exudate (ACWE) medium, elaborated virulence factors and metabolisms that may be relevant *in vivo*. For example, *P. aeruginosa* biofilms produced phenazines, quorum-sensing-regulated proteases, and systems for acquisition of iron and zinc. *P. aeruginosa* biofilm cells expressed genes consistent with hypoxia (52), including those for denitrification and pyruvate metabolism. *A. baumannii* biofilms robustly expressed a pathway that degrades

Downloaded from https://journals.asm.org/journal/aac on 19 April 2022 by 153.90.118.208.

TABLE 4 Gene sets differentially expressed between biofilm and planktonic conditions[a]

P. aeruginosa and expression direction in biofilm	*A. baumannii*	*S. aureus*
Up		
Stationary phase	**Stationary phase**	**Stationary phase**
NO_3^-/NO_2^-/NO metabolism	Phenylacetic acid degradation	**Iron acquisition**
Phenazine biosynthesis	Antibiotic resistance	Host binding/virulence
HSL quorum sensing	Valine degradation	**Pyruvate/Ser/Ala fermentation**
Pyochelin biosynthesis (iron)	PNAG synthesis	Superantigen-like proteins
Bacteriophage Pf1	Trehalose synthesis	**Zn transport**
Type IV pili		**NO_3^-/NO_2^-/NO metabolism**
ClpA/B		Leukotoxins/lysins
Zn transport/Zn limitation		Pro, His, Arg catabolism
Pyruvate fermentation		Lantibiotic
Oxidative stress		Arginine deiminase pathway
		Sae regulatory
		Peptidoglycan recycling
Down		
Ribosome	Amino acid transport	DNA synthesis/topoisomerase
Purine metabolism	Oxidative stress	**Lysine biosynthesis**
Amino acid—tRNA ligase	Pilus related	Leucine biosynthesis
DNA replication		Competence
Cys/Met biosynthesis		Peptide transport
NADH-quinone oxidoreductase		**Cys/Met biosynthesis or uptake**
Lipopolysaccharide		**Amino acid-RNA ligase**
Tricarboxylic acid cycle		Queuosine synthesis
ATP synthase		
PQS biosynthesis		
Fatty acid biosynthesis		
Cobalamin biosynthesis		
EMP pathway		
Histidine biosynthesis		
Peptidoglycan synthesis		
Arginine biosynthesis		
Vitamin B_6 metabolism		
Lysine biosynthesis		
Pyrimidine metabolism		
Riboflavin		
RNA polymerase		

[a]Boldface indicates a gene set that was differentially expressed in more than one microorganism.

phenylacetic acid (67), a response that has been shown to diminish neutrophil recruitment *in vivo* (69). *S. aureus* biofilms expressed systems for acquiring iron and zinc and made numerous known host-binding proteins, leukotoxins, and other virulence factors. *S. aureus* biofilms exhibited metabolic shifts toward fermentation of pyruvate, serine, and alanine, denitrification, and the arginine deiminase pathway. These physiologies were expressed even though ACWE contains no host cells or host factors. We compared the genes increasingly expressed in our *S. aureus* drip-flow biofilms (count, 449) to the gene list reported by Xu et al. (70) to be upregulated in a human prosthetic joint infection (count, 232). There were 128 genes that overlapped, a highly significant commonality ($P < 10^{-14}$). Indeed, this overlap is at least as strong as the overlap between our *S. aureus* biofilm and other *in*

TABLE 5 Bacterial biofilms express genes associated with stationary phase[a]

Organism	No. of genes upregulated in SP	No. of genes upregulated in biofilm	No. of genes on both lists	*P* value for overlap
P. aeruginosa	120	449	85	$<10^{-15}$
A. baumannii	37	259	17	4×10^{-11}
S. aureus	283	232	75	$<10^{-15}$

[a]For each microorganism, a list of genes that are expressed at higher levels in stationary-phase (SP) compared to exponential-phase planktonic cultures was compiled from published literature (see the supplemental material). The overlap between these lists and the genes expressed at higher levels in biofilms compared to planktonic cultures in this study was determined.

Downloaded from https://journals.asm.org/journal/aac on 19 April 2022 by 153.90.118.208.

TABLE 6 Gene sets differentially expressed between antibiotic-treated biofilm and untreated biofilm conditions[a]

P. aeruginosa **and increase/decrease in expression in treated biofilm**	***A. baumannii***	***S. aureus***
Up		
Bacteriophage Pf1	Benzoate degradation	Cell wall stress
Purine metabolism	DNA metabolism	
SOS response	Malonate metabolism	
Cell wall synthesis/shape	Iron-Sulfur protein	
Amino acid tRNA ligase	Arsenic resistance	
Glyoxylate shunt	Adipic acid degradation	
	PNAG synthesis	
Down		
Protein secretion-T6SS	**Iron acquisition**	Possible phage
HSL quorum sensing	NADH-quinone oxidoreductase	
Phenazine biosynthesis	TCA cycle	
Pyochelin biosynthesis (iron)	**Pilus related**	
Type IV pili	Cytochromes	
Pyoverdine biosynthesis (iron)	ATP synthase	
	Fatty acid oxidation	
	Valine degradation	
	Phenylacetic acid degradation	

[a]Boldface indicates a functional group that appears on more than one list.

vitro biofilm investigations (71–74). This leads us to hypothesize that substantial features of the *in vivo* bacterial phenotype are manifest in response to *in vitro* growth as a biofilm on a medium that simulates the *in vivo* chemical microenvironment (75, 76).

Genes differentially expressed between untreated biofilm and antibiotic-treated biofilm. Exposure of biofilms to antibiotics resulted in changes in gene expression in all three of the biofilms examined (Table 3). We wondered if some of the changes observed were the same between the three microbial species, as these shared genes could represent a common biofilm-specific protective mechanism. Transcripts changing at least 2-fold at a P value of <0.05 in response to the addition of antibiotics were selected for use in this analysis. However, when the same validated OrthoFinder analysis was performed, no similar responses in gene regulation to antibiotics was found in the three species. There were no orthogroups found to be upregulated or downregulated in all three species in response to antibiotic treatment.

Inspecting identified functional groups of genes that change in response to antibiotic treatment (Table 6) revealed possible decreases in expression of genes associated with iron acquisition and pili in both *P. aeruginosa* and *A. baumannii*. No gene functional category was shared across the three bacteria when exposed to antibiotic.

Metabolomic comparison of biofilm and planktonic cells and of untreated biofilm and antibiotic-treated biofilm. The utilization and production of extracellular metabolites was compared between planktonic and untreated biofilm systems to identify possible common changes in cellular metabolism between the two growth modes. Extracellular metabolomic analyses were performed to determine concentrations of 18 amino acids, lactate, glucose, acetate, formate, and ethanol in the supernatant of planktonic cultures and effluent of biofilm reactors. The amount of each substrate consumed or metabolic product produced was normalized by the total carbon utilized by each system. Results of this analysis for *P. aeruginosa* were previously published (52).

All three bacteria consumed glucose, lactate, and amino acids in both planktonic and biofilm growth modes. *P. aeruginosa* produced acetate as a metabolic product during biofilm growth, and *S. aureus* biofilms produced acetate, formate, and ethanol. Neither organism produced detectable amounts of these products in planktonic growth. There was net production of some amino acids during biofilm growth of *A. baumannii* and *S. aureus*. Across the three species, the only metabolites whose normalized utilization changed consistently (in the same direction and by a fold change of 1.5 or greater) were glucose, alanine, and aspartic acid (Table 7). Glucose consumption was increased in biofilms compared to planktonic cells, and alanine and aspartic acid utilization was decreased in biofilms compared to planktonic cells.

Downloaded from https://journals.asm.org/journal/aac on 19 April 2022 by 153.90.118.208.

TABLE 7 Fold changes in normalized metabolite utilization that were in the same direction for all three bacterial species and greater than 1.5-fold different between the planktonic and untreated biofilm conditions[a]

Organism	Glucose	Alanine	Aspartic acid
P. aeruginosa	9.6	0.64	0.50
A. baumannii	1.9	0.42	0.28
S. aureus	2.2	0.26	0.63

[a]Values greater than 1 indicate higher relative consumption in the biofilm than the planktonic condition. Values less than 1 indicate lower relative consumption in the biofilm compared to planktonic conditions.

The same extracellular metabolomic analysis was performed to characterize shifts in metabolism between control (untreated) biofilms and biofilms treated with antibiotics for 24 h. Overall trends in the cumulative utilization of substrates and excretion of metabolic products are summarized in Table 8. Treatment of *P. aeruginosa* biofilms with antibiotic had no effect on the combined uptake of lactate, glucose, and amino acids. Antibiotic treatment of the biofilm reduced acetate production (the sole metabolic product detected in this analysis for *P. aeruginosa*). *A. baumannii* biofilms exhibited a 36% decrease in substrate utilization after antibiotic treatment. Treatment of *S. aureus* biofilms with antibiotic reduced the combined uptake of carbonaceous substrates by 66% and reduced the excretion of products by 30%.

Note that the reductions in substrate utilization were much smaller than the reductions in viable cell counts (Table 1). For example, viable cells in *P. aeruginosa* biofilms treated with ciprofloxacin were reduced by 99%, but there was no change in overall substrate uptake. *A. baumannii* biofilms treated with tigecycline exhibited an 85% reduction in viable cells but only a 36% reduction in substrate uptake. For *S. aureus* biofilms treated with daptomycin, viable cells were reduced by 96% compared to the 66% reduction measured in overall substrate uptake. These comparisons suggest that even though antibiotic-exposed cells from a biofilm have lost the ability to form a colony on a plate, they may continue to manifest metabolic activities. There were no consistent patterns of relative metabolite utilization or production that were the same for all three organisms when comparing untreated with antibiotic-treated biofilms.

DISCUSSION

One of the most consistently described phenotypic characteristics of microbial biofilms is tolerance to antimicrobial agents of all kinds (1–5). Given this nearly universal protection in the biofilm state compared to planktonic cells, it is reasonable to hypothesize that there is a common genetically encoded basis for this defense. We sought to uncover evidence of such a shared tolerance gene, gene set, or pathway by investigating three bacterial species, each grown as single-species biofilms under conditions that simulated the chemical and physical environment in a human chronic dermal wound. These conditions included a synthetic medium containing lactate, glucose, and a cocktail of amino acids, an air interface across which oxygen could be transferred, a representative temperature (33°C), and a slow continuous flow of the medium. The three microorganisms represent two Gram negatives (*P. aeruginosa* and *A. baumannii*) and a Gram positive (*S. aureus*). Each biofilm was challenged with an antibiotic appropriate to the microorganism. The three drugs represented three distinct classes

TABLE 8 Utilization of substrates and excretion of products by untreated biofilms and antibiotic-treated biofilms[a]

	Substrate utilization		Product excretion	
Organism	Biofilm	Treated biofilm	Biofilm	Treated biofilm
P. aeruginosa	49.7	49.9	2.8	0.9
A. baumannii	34.3	22.0	4.9	5.5
S. aureus	32.6	14.3	11.6	8.2

[a]Concentrations are given as mM carbon.

Downloaded from https://journals.asm.org/journal/aac on 19 April 2022 by 153.90.118.208.

of antibiotics: a fluoroquinilone, a tetracycline, and a cyclic lipopeptide. We reasoned that if a robust and consistent gene-based defense mechanism exists, it should be discernible across a variety of species and also for diverse antibiotics. Although antibiotic-specific responses are certainly anticipated, the conjecture we are testing in this work is that there is a biofilm-specific response to stress that is universal across organisms. By keeping the growth conditions the same, we reduced variations due to changes in experimental conditions. All three bacteria were less susceptible to killing by antibiotics when grown as biofilms compared to planktonic cells (Table 1). This result accords with many prior reports using these bacterial species (5–43).

Our first prediction was that there would be a shared set of conserved genes expressed in the same differential fashion between planktonic and biofilm bacteria for the three organisms. We did not find any such gene set shared across the three species. A single orthogroup was common in the biofilm-upregulated genes of the trio of bacteria, a degree of overlap too small to be considered statistically significant. Four orthogroups were shared in the genes downregulated in biofilms, also a degree of overlap that did not reach statistical significance. When the requirement for strict gene conservation was relaxed to examine shared functions (prediction number ii from the Introduction), we identified only a single functional category of genes, those associated with the transition from exponential to stationary phase, that was common to all three microorganisms. Several functions were shared by *P. aeruginosa* and *S. aureus*, including indications of increased denitrification and pyruvate fermentation in biofilms compared to planktonic cells. Both of these functions are plausible adaptive responses to oxygen limitation in the biofilm. Both *P. aeruginosa* and *S. aureus* also expressed genes associated with iron sequestration and zinc transport, suggesting that these metals become scarcer in the biofilm mode of growth. Clear evidence of quorum-sensing activity in the biofilm was found for only one of the three bacteria, *P. aeruginosa*.

The second prediction following from our hypothesis was that there would be a shared transcriptomic response to antibiotic exposure across the three species. We found no examples of shared genes by sequence homology, neither upregulated or downregulated, across the three microorganisms. The related prediction (number iv) that common functional groups rather than specific genes occur in response to antibiotics was evaluated by manually curating genes into functional groups. No functional group common to all three bacteria could be identified. If we had used an antibiotic from the same class for all three microorganisms, we would have expected to find some commonalities among the transcriptomic responses to the drug. We would also predict that these responses would be similar to known responses that have been described in planktonic cells; this was indeed the case. For example, prior work with ciprofloxacin-treated *P. aeruginosa* has reported induction of genes involved in the SOS response (77–79), and we also observed upregulation of this gene set. Prior work with daptomycin-treated *S. aureus* has reported induction of genes associated with cell wall stress (80, 81), which we also measured. Hua et al. (82) reported suppression of the aerobic phenylacetate catabolic pathway after exposure of *A. baumannii* to tigecycline, and we also identified this behavior. By using antibiotics from different classes, we sought to discover biofilm-specific tolerance mechanisms that are distinct from known responses to particular antibiotics. Again, no such gene set could be discerned.

A limitation of our transcriptomic approach is that it cannot identify changes that are posttranscriptionally or posttranslationally regulated. For example, extracellular polysaccharide synthesis in biofilm can be regulated both at the transcriptional and at the posttranscriptional level (83) with the secondary messenger molecule cyclic-di-GMP, which is required for synthesis of some extracellular polysaccharides (84–87).

Our third prediction was that there could be a consistent shift, across the three bacteria, in the pattern of consumption of metabolic substrates either between the biofilm and planktonic growth modes or between the antibiotic-treated biofilm and untreated biofilm conditions. Biofilm microorganisms did consistently consume more glucose (as a percentage of total carbon utilization) than planktonic cells. One possible explanation for this shift

Downloaded from https://journals.asm.org/journal/aac on 19 April 2022 by 153.90.118.208.

is an increased synthesis of extracellular polysaccharides starting from glucose in biofilm cells. Of the three bacteria, only *A. baumannii* revealed an upregulation at the transcriptional level of polysaccharide biosynthetic genes in biofilms. The decreased utilization of alanine and aspartic acid in biofilms compared to planktonic cells was not evident in the transcriptomic comparisons.

Overall, our measurements do not support the existence of a shared genetic or biochemical basis for biofilm tolerance against antibiotics across bacterial species. Rather, each microorganism appears to exhibit distinct patterns of gene expression and functional shifts in response to growth in a biofilm and subsequent antibiotic treatment. We hypothesize that multitudinous and redundant molecular mechanisms have evolved that implement tolerance in biofilms and that these vary by taxa and even by strain. The variety of these mechanisms and their possible redundancy would underpin a very robust defense. Thus, there is likely no common molecular Achilles' heel for all biofilms.

Susceptibility testing of defined genetic mutants for defects in biofilm tolerance to antibiotics is a powerful experimental approach that we did not use in this study but that we and others have used previously. A wide variety of mutations in genes that reduced antibiotic tolerance have been identified (1, 11, 12, 14, 15, 17–22, 24, 39, 52, 88–99), but only a couple of recurrent themes emerge from studies reproduced in more than one laboratory. In *P. aeruginosa*, biofilms formed by mutants deficient in synthesis of varied extracellular polysaccharides are often more susceptible to killing by antibiotics (52, 91, 93–98). The stringent response, mediated by the alarmone ppGpp, has been shown to contribute to biofilm defense in *P. aeruginosa*, *S. aureus*, and *Enterococcus faecium* (14, 20, 52, 100, 101).

We propose the following general conceptual model for how antibiotic tolerance manifests in biofilms (52). In the earliest stages of biofilm formation, there is little change in the chemical microenvironment because cell aggregates are small. Diffusion is rapid enough over these short distances that oxygen and other metabolic substrates fully permeate biofilm structures (102). Metabolic products are likewise readily cleared from the biofilm by diffusion. In this early phase, microbial cells exhibit rapid growth and relatively high antibiotic susceptibility (2). As biofilm aggregates increase in size, reaction-diffusion interactions lead to the development of gradients in the concentrations of metabolic substrates and products (54). Metabolic substrates are at reduced concentrations in the biofilm interior, whereas metabolic products are at elevated concentrations in the biofilm interior. This chemical heterogeneity causes shifts in the metabolism and gene expression of the microorganisms as the bacteria respond to the local microenvironment (16, 38, 44, 45). These changes could include, for example, (i) depletion of oxygen, leading to induction of responses to hypoxia and shifts to denitrification or fermentation pathways, (ii) increased synthesis of extracellular polymeric substances, (iii) increased relative consumption of sugar substrates to support synthesis of extracellular polysaccharides, (iv) depletion of metal cations as they are sequestered by binding to extracellular polymeric substances or utilized for cellular enzymes, (v) induction of systems to acquire depleted metal cations, and (vi) accumulation of quorum-sensing molecules leading to increased biosynthesis of quorum-sensing controlled products. As local chemical conditions persist or exacerbate, additional stress responses might be induced, for example, (i) acid stress in response to accumulation of fermentation end products such as carboxylic acids that lower the local pH, (ii) oxidative stress due to unbalanced metabolisms, and (iii) starvation stress responses. Sustained substrate limitation is expected to result in these possible outcomes: (i) reduced anabolism and diminished expression of cellular machinery for transcription, translational, and replication, (ii) reduced specific growth rates, including enrichment of nongrowing cells, and (iii) entry of some cells into protected dormant states, possibly involving ribosome hibernation (103–105). This collection of hypothesized physiological changes occurs prior to antibiotic treatment and leads to biofilms cells occupying a spectrum of states all of which have the potential to contribute to antibiotic tolerance. Finally, antibiotic exposure is expected to induce adaptive responses that further enhance antibiotic tolerance (11, 106, 107).

MATERIALS AND METHODS

Bacterial strains and culture medium. *P. aeruginosa* PAO1 (108), *Staphylococcus aureus* USA300 FPR3757 (109, 110), and *Acinetobacter baumannii* AB5057 (111) were cultured individually using a medium

Downloaded from https://journals.asm.org/journal/aac on 19 April 2022 by 153.90.118.208.

designed to mimic the exudate from a human chronic wound (52), referred to as artificial chronic wound exudate (ACWE) medium. ACWE was composed of basal salts, amino acids, L-lactate, glucose, $MgCl_2$, $CaCl_2$, thiamine, nicotinic acid, and $FeSO_4$, adjusted to pH 7.5, as described in Stewart et al. (52). When used, antibiotics were added at these final concentrations: ciprofloxacin, 1 mg/liter; daptomycin, 10 mg/liter; tigecycline, 20 mg/liter. Some of the data from *P. aeruginosa* experiments have been published previously (52).

Planktonic culture conditions. Planktonic cultures were prepared by inoculating 100 mL of ACWE medium with 1 mL of an overnight culture in 500-mL baffled Erlenmeyer flasks. Cultures were incubated to early exponential phase for each species (optical density [OD] of 0.25, 1×10^8 CFU mL^{-1} for PAO1; OD of 0.50, 3×10^8 CFU mL^{-1} for AB5075; and OD of 0.10, 1.3×10^8 CFU mL^{-1} for USA300) at 33°C (the approximate surface temperature of a dermal wound). Cells were harvested by centrifugation at $5{,}125 \times g$ for 5 min at 4°C in an Allegra X-15R centrifuge (Beckman Coulter, Brea, CA) and frozen at −80°C for use in metabolomic and transcriptomic studies. A minimum of three independent biological replicates was performed for each species.

To measure killing of suspended cells, planktonic cultures of *P. aeruginosa* and *A. baumannii* were prepared by inoculating 0.5 mL of overnight cultures into 25 mL of ACWE medium in 250-mL baffled Erlenmeyer flasks. For *S. aureus*, a colony from an overnight plate was used to inoculate the medium. The cultures were incubated until reaching an optical density of 0.20 to 0.50 (early logarithmic phase) at 33°C on an orbital shaker at 200 rpm. The cultures were then serially diluted in phosphate-buffered saline (PBS) and plated on tryptic soy agar (TSA) to determine initial bacterial density. Each culture was then divided into two 10-mL aliquots and one was treated with antibiotic, leaving the other as a control. Antibiotics and treatment concentrations were as given in Table 1. The treated and control cultures were then incubated statically at 33°C for 24 h. The cultures were then serially diluted in PBS and plated on TSA to determine final bacterial density.

Biofilm growth conditions. Biofilms were grown as described in Stewart et al. (52) (see Fig. S1 in the supplemental material). Briefly, biofilms were cultivated on hydroxyapatite-coated glass slides (Clarkson Chromatography, South Williamsport, PA) in a drip-flow reactor (DFR) designed by Biosurface Technologies Corp., Bozeman, MT (112). Five milliliters of exponential-phase culture in ACWE was added to each channel of the DFR and incubated for 1 h at 33°C to allow for cell attachment. Following the batch phase, a MasterFlex L/S model 7519-20 peristaltic pump (Cole-Parmer, Vernon Hills, IL) was started at a flow rate of 10 mL/h, and biofilms were cultivated at 33°C for 72 h. ACWE medium containing the organism-specific antibiotic was then pumped through the treatment chambers, while ACWE without antibiotic continued to flow through the untreated control chambers for 24 h. After a total of 96 h of growth, biofilms were harvested by scraping into 10 mL phosphate-buffered saline (PBS). The cell suspension was homogenized by vortexing and passage through an 18-gauge, 1.5-inch-long Precisionglide needle (Beckton Dickinson and Co., Franklin Lakes, NJ). Cell pellets were collected by centrifugation and placed in a −80°C freezer. A minimum of three biological replicates were performed with each species.

Quantification of protein, carbohydrates, and DNA in biofilms. Total protein in biofilm samples was quantified by the Bradford assay (113) as described in reference 52. Total carbohydrates from biofilm samples were quantified using the phenol-sulfuric acid described in reference 114, with modifications for total carbohydrate analysis of biofilms described in reference 50. D-(+)-galactose (Sigma-Aldrich, St. Louis, MO) was used to generate standard curves. DNA was isolated and quantified from *Pseudomonas aeruginosa* and *Acinetobacter baumannii* biofilm samples using the QIAamp miniprep kit (Qiagen, Germantown, MD) as described in Stewart et al. (52). To isolate DNA from *Staphylococcus aureus* biofilms, cell pellets were resuspended in a solution of Tris-EDTA (TE) containing 0.5 mg/mL lysostaphin (AMBI Products, LLC, Lawrence, NY) and 3.0 mg/mL lysozyme (Millipore Sigma, Burlington, MA). Following a 60-min incubation, DNA extraction was carried out with the QIAampDNA minikit (Qiagen, Germantown, MD) according to the manufacturer's instructions, with an RNase A treatment to obtain RNA-free genomic DNA. DNA was measured on a NanoDrop 1000 (Thermo Fisher Scientific, Waltham, MA) a minimum of three times for each biological sample.

Preparation of RNA. RNA was previously extracted, purified, and quantified from *Pseudomonas aeruginosa* planktonic, biofilm, and treated biofilm cells as described in Stewart et al. (52). RNA extraction from *Acinetobacter baumannii* samples proceeded similarly. Briefly, frozen *Acinetobacter baumannii* cell pellets were resuspended in 100 μl TE-lysozyme, with the lysozyme concentration at 5 mg mL^{-1}. Following a 3-min room temperature incubation, Tri-reagent (Zymo Research, Irvine, CA) was added and the samples were further incubated for 5 min at room temperature. After the addition of an equal volume of 100% ethanol, the mixture was applied to a Zymo-Spin IIC column. RNA extraction was performed using the Direct-Zol Mini-Prep kit (Zymo Research, Irvine, CA) per the manufacturer's instructions, including an on-column DNase treatment. Samples were then treated with Turbo DNase (Thermo Fisher Scientific, Waltham, MA) by following the rigorous treatment protocol in the presence of 1 μl of RnaseIn Plus (Promega, Madison, WI). Next, samples were applied to Clean and Concentrator-25 columns (Zymo Research, Irvine, CA) by following the manufacturer's procedure for recovery of total RNA greater than 200 nucleotides in size.

RNA extraction from *Staphylococcus aureus* was modified slightly to increase lysis efficiency from this Gram-positive organism. Briefly, cell pellets from planktonic cultures, biofilms, and treated biofilms were incubated for 2 min at 37°C in TE, pH 8.0, containing 0.5 mg/mL lysostaphin and 3.0 mg/mL lysozyme with frequent vortexing. Following the addition of 1 mL of Tri-reagent (Zymo Research, Irvine, CA), samples were incubated for 5 min at room temperature and then for 5 min at 65°C with vortexing. After the addition of an equal volume of 100% ethanol, the mixture was applied to a Zymo-Spin IIICG column. RNA extraction was performed using the Direct-Zol Mini-Prep kit (Zymo Research, Irvine, CA) per the manufacturer's instructions, including on-column DNase treatment. Samples were then treated with Turbo DNase (Thermo Fisher Scientific, Waltham, MA) by following the rigorous treatment protocol in the presence of 1 μl of RnaseIn Plus (Promega, Madison, WI). Next, samples were applied to Clean and Concentrator-25 columns (Zymo Research, Irvine, CA) by following the manufacturer's procedure for

Downloaded from https://journals.asm.org/journal/aac on 19 April 2022 by 153.90.118.208.

recovery of total RNA greater than 200 nucleotides in size. For all samples, RNA quality was assessed on the BioAnalyzer 2100 (Agilent, Santa Clara, CA) RNA6000 nano-assay.

Microarray analysis. *Pseudomonas aeruginosa* RNA samples were prepared and hybridized to Affymetrix (now ThermoFisher Scientific, Waltham, MA) *P. aeruginosa* microarrays (part 900339) previously (50).

Staphylococcus aureus RNA samples (10 μg) were also reverse transcribed, fragmented, and labeled according to the Affymetrix prokaryotic target labeling protocol (GeneChip expression analysis technical manual, November 2004). Labeled cDNA was then hybridized to GeneChip *S. aureus* genome arrays (part 9003514; Applied Biosystems, ThermoFisher Scientific, Waltham, MA) for 16 h at 45°C with constant rotation. Microarrays were stained using a GCOS Fluidics Station 450 and scanned with an Affymetrix 7G scanner. Affymetrix GCOS v1.4 was used to generate CEL files, which were imported into FlexArray v1.6.1 for quality control and data analysis.

Acinetobacter baumannii RNA samples were prepared for custom microarrays for *Acinetobacter baumannii* 5075 designed and manufactured by MYcroarray (now Arbor Biosciences, Ann Arbor, MI) in the following manner. Random hexamer primers (1 μl; Invitrogen, now ThermoFisher Scientific, Waltham, MA) were annealed to 9 μg of RNA in the presence of 1 μl RNaseIn Plus (Promega, Madison, WI) during a 10-min 70°C incubation. After a 30-s incubation on ice, RNA was reverse transcribed at 42°C overnight using the following reagents from Invitrogen (now ThermoFisher Scientific, Waltham, MA): 5.5 μl 5$\times$ first-strand buffer, 3 μl 0.1 M dithiothreitol (DTT), 0.6 μl 25 mM modified deoxynucleotide triphosphate (dNTP) mix (2:1 ratio of amino-allyl dUTP to dTTP), and 2 μl Superscript II. After synthesis, the remaining RNA was hydrolyzed by the addition of 0.5 M EDTA and 1 N sodium hydroxide at 70°C for 15 min. Next, resulting cDNA samples were neutralized with 1 N HCl and applied to Clean and Concentrator-25 columns (Zymo Research, Irvine, CA) according to the manufacturer's instructions, with the substitution of a modified wash buffer (5 mM KPO_4, 80% ethanol) as specified in SOP#M007 (JCVI, Rockville, MD). The resulting cDNA was assessed for quantity and purity with a NanoDrop 1000 (ThermoFisher Scientific, Waltham, MA). It was then dried to completion for 30 min without heat in an RC10.10 Vacufuge (Jouan, Inc., Winchester, VA) and resuspended in 5 μl sodium carbonate buffer, pH 9.3. Each cDNA sample was labeled with Cy 3 dye (GE Healthcare, Chicago, IL) for a minimum of 90 min at room temperature, protected from light, with mixing every 30 min. The reaction was quenched with 40 μl 0.1 M sodium acetate, pH 5.2. Unincorporated dye molecules were removed with Clean and Concentrator-25 columns (Zymo Research, Irvine, CA). Quantities and incorporation rates were assessed with a NanoDrop 1000 (ThermoFisher Scientific, Waltham, MA). Samples hybridized to microarrays contained a minimum of 1,500 pmol Cy dye and 4 μg cDNA. Custom microarrays were designed by MYcroarray (now Arbor Biosciences, Ann Arbor, MI) specifically for *Acinetobacter baumannii* AB5075, with 5 replicate probes for every transcript. Four independent biological replicates were performed for each of the three conditions, for a total of 12 microarrays. A hybridization mixture containing 6$\times$ saline sodium phosphate EDTA buffer (SSPE), 20% formamide, 0.12 mg acetylated bovine serum albumin (BSA), 0.02% Tween 20, 1% MYcroarray control oligonucleotides, 10 μg salmon sperm, and 4 μg cDNA in a 130-μL final volume was prepared for each sample. This was mixed, incubated at 65°C for 5 min, and then kept on ice for 5 min. The hybridization chamber (G2534A; Agilent), gasket slide (G2534-60011; Agilent Technologies), and MYcroarray slide (custom slide array CAT-3x20k-*Acinetobacter*_baumannii_AB5075) were preheated to 65°C. Samples were hybridized to the microarray for 18 h at 48°C and secured to the front of a culture roller with constant vertical rotation at 1.7 rpm. Array slides were then liberated from the gasket slide in 1$\times$ SSPE and washed with gentle agitation on a rocker (Boekel Scientific, Feasterville, PA). The washes were performed with 1$\times$ SSPE at room temperature for 3 min, 1$\times$ SSPE at room temperature for 3 min, 1$\times$ SSPE at 48°C for 3 min, and then 0.25$\times$ SSPE at room temperature for 30 s. The slides were spun for 1 min in a high-speed microarray centrifuge (ArrayIt Corporation, Sunnyvale, CA). Image acquisition was performed on the GenePix 4000B scanner (Molecular Devices, San Jose, CA) at 532-nm wavelength, a PMT gain of 600, 100% laser power, and pixel size of 5, with averaging of 3 lines. Resulting images were saved as tiff files and converted to intensity values with GenePix Pro v6.1 software.

Transcriptomic data analysis. *Pseudomonas aeruginosa* microarray data from three independent biological replicates from each condition (planktonic, biofilm, and treated biofilm) was background corrected and normalized using the GC-RMA algorithm in Flexarray 1.6.1 as published in Stewart et al. (52). Analysis of variance (ANOVA) was performed to determine genes with statistically significant changes in expression (2-fold change at a P value of $<$0.05).

Staphylococcus aureus microarray data from three independent biological replicates was processed in the same manner to identify genes with statistically significantly changes in expression between the conditions at 2-fold change and a P value of $<$0.05. Strain USA300_FPR3757 was hybridized to Affymetrix *S. aureus* microarrays that contain probes designed for the following four strains: N315, Mu50, NCTC 8325, and COL. To interpret the data, Affymetrix identifiers (IDs) from the four strains were converted to USA300 gene IDs based on PanGenome identifiers from AureoWiki, the repository of the *Staphylococcus aureus* research and annotation community (115). USA300_FPR3757 has 2,639 PAN IDs, and there are 91 genes completely unique to USA300, which were not represented on the arrays. Therefore, the final resulting data contain a concise list of USA300 identifiers most similar to the sequences present on the array, representing approximately 89% coverage of strain USA300_FPR3757 open reading frames.

Gpr files of *Acinetobacter baumannii* array data were imported into Flexarray v.1.6.1, where local background correction and quantile normalization were performed. Resulting normalized median pixel intensity values for each probe were exported to Excel, where the trimmed mean was calculated and combined with annotation obtained from MYcroarray, PATRIC, NCBI, and the Manoil group. Trimmed means were reimported in to Flexarray 1.6.1, and ANOVA was performed to determine differentially expressed gene at a P value of $<$0.05 and fold change of $>$2.

Downloaded from https://journals.asm.org/journal/aac on 19 April 2022 by 153.90.118.208.

OrthoFinder analysis. We used OrthoFinder to identify orthologs, paralogs, and orthogroups from the protein sequences of the three species. OrthoFinder (version 2.4.1) was downloaded at https://github.com/davidemms/OrthoFinder. The main parameters of OrthoFinder were set as follows. The sequence search program was set to diamond, the method for gene tree inference was set to dendroblast, and the MCL inflation parameter was set to 1.5. Orthogroups in common were identified using Excel version 2102 and Venny 2.1 (116).

Overlap analysis. Gene set enrichment analysis was performed by determining the overlap between the gene lists from this study and gene lists compiled from the literature as described previously (20). *P* values for assessing the statistical significance of gene set enrichment were calculated using a negative binomial distribution.

Analysis of extracellular metabolites by gas chromatography-mass spectrometry (GC-MS). Extracellular metabolite samples from biofilms were collected from DFR effluent lines into 15-mL Falcon tubes (Corning Inc., Corning, NY). Collection lines were unclamped and allowed to drain for approximately 1 h. Samples were capped and placed in a −80°C freezer. After biofilms were harvested, stock medium and ciprofloxacin-containing medium were collected in 50-mL Falcon tubes and frozen at −80°C. Extracellular metabolites from planktonic cultures were collected by decanting and freezing the supernatant from the pelleting process. Extracellular metabolite samples were thawed, and 1-mL aliquots were dried under a nitrogen stream. Prior to analysis, samples were derivatized using the method described below that enabled the consistent detection of 17 amino acids and three central carbon metabolites. Two additional central carbon metabolites, formate and acetate, were detected as underivatized compounds in aqueous solution using a ZB-WAX column.

N-tert-Butyldimethylsilyl-*N*-methyltrifluoroacetamide (MTBSTFA) was obtained from Sigma (CAS 77377-52-7; Sigma-Aldrich, Switzerland). Acetonitrile (ACN) solvent was obtained from Fisher (CAS 75-05-8; Fisher Scientific). Hexanes solvent was obtained from Fisher (CAS 110-54-3). Formic acid and acetic acid were obtained from Fisher. The remaining central carbon metabolites were obtained from Sigma. All amino acids were purchased from Sigma.

Analysis of samples was carried out using an Agilent 7890A GC oven system, coupled to an Agilent 5975C inert XL EI/CI MSD with triple-axis detector mass spectrometer. Sample organization and injection was performed by an Agilent 7693 Autosampler.

For the analysis of amino acids and central carbon metabolites, aqueous solutions previously dried using nitrogen were resuspended in ACN and derivatized using MTBSTFA. Equal volumes of MTBSTFA and ACN (100 μL) were added to each sample in a glass GC vial, capped, vortexed briefly, and then incubated on a hot plate at 50°C for 30 min. Derivatized samples were transferred to new GC vials containing glass inserts for analysis. Separation of analytes was accomplished with a Phenomenex Zebron ZB-5MS nonpolar column (30 m by 0.25 mm inner diameter, 0.25 μm) The GC temperature gradient for the MTBSTFA-derivatized samples was 60°C for 2 min, ramping to 120°C at a rate of 20°C/min (3 min ramp time) and then to 155°C at a rate of 6°C/min (5.83 min ramp time), and finally ramping to a temperature of 300°C at a rate of 14.5°C/min (10 min ramp time), where the temperature was held for 10 min. The total run time was 30.833 min. Helium gas was used as the carrier at a flow rate of 1.5 mL/min. Injections were performed at a volume of 1 μL, with a split ratio of 10:1, and an inlet temperature of 325°C. The interface temperature between the GC and MS was set at 230°C. The volatile central carbon metabolites, formate and acetate, were analyzed underivatized in aqueous solution. Analysis was performed using a Phenomenex Zebron ZB-WAX column (30 m by 0.25 mm inner diameter, 0.50 μm). The oven temperature started at 75°C and was held for 1 min. It was then ramped at a rate of 6°C/min to 180°C (17.5 min ramp time) and then ramped at 10°C/min to 230°C (5 min ramp time), where it was held for 5 min. The total run time was 28.5 min. Helium gas was used as a carrier at a flow rate of 3 mL/min. Injections were performed at a volume of 0.5 μL, splitless, with the inlet temperature set at 240°C and the interface temperature set at 280°C.

Glucose was determined using an enzymatic kit (GAGO-20, KA-1652, and AA0100; Sigma, St. Louis, MO).

Data availability. The raw data derived from these analyses have been deposited in the Gene Expression Omnibus database with accession number GSE186080.

SUPPLEMENTAL MATERIAL

Supplemental material is available online only.

SUPPLEMENTAL FILE 1, PDF file, 0.2 MB.

SUPPLEMENTAL FILE 2, XLSX file, 0.1 MB.

SUPPLEMENTAL FILE 3, XLSX file, 0.1 MB.

SUPPLEMENTAL FILE 4, XLSX file, 0.03 MB.

SUPPLEMENTAL FILE 5, XLSX file, 0.03 MB.

SUPPLEMENTAL FILE 6, XLSX file, 0.04 MB.

ACKNOWLEDGMENTS

Funding for the Proteomics, Metabolomics, and Mass Spectrometry Facility used in this publication was made possible in part by the MJ Murdock Charitable Trust, the National Institute of General Medical Sciences of the National Institutes of Health under award numbers P20GM103474 and S10OD28650, and the MSU Office of Research, Economic Development and Graduate Education. The content is solely the responsibility of the authors and does not necessarily represent the official views of the National Institutes of Health.

Downloaded from https://journals.asm.org/journal/aac on 19 April 2022 by 153.90.118.208.

This was not an industry-supported study. The authors have indicated no financial conflicts of interest. The opinions and assertions contained here are the private views of the authors and are not to be construed as official or as reflecting the views of the U.S. Army, the U.S. Department of Defense, or the Henry M. Jackson Foundation for the Advancement of Military Medicine, Inc. This paper has been approved for public release with unlimited distribution.

REFERENCES

1. Mah TF, Pitts B, Pellock B, Walker GC, Stewart PS, O'Toole GA. 2003. A genetic basis for *Pseudomonas aeruginosa* biofilm antibiotic resistance. Nature 426:306–310. https://doi.org/10.1038/nature02122.
2. Stewart PS. 2015. Antimicrobial tolerance in biofilms. Microbiol Spectr 3: MB-0010-2014. https://doi.org/10.1128/microbiolspec.MB-0010-2014.
3. Yan J, Bassler BL. 2019. Surviving as a community: antibiotic tolerance and persistence in bacterial biofilms. Cell Host Microbe 26:15–21. https://doi.org/10.1016/j.chom.2019.06.002.
4. Crabbé A, Jensen PØ, Bjarnsholt T, Coenye T. 2019. Antimicrobial tolerance and metabolic adaptations in microbial biofilms. Trends Microbiol 27:850–863. https://doi.org/10.1016/j.tim.2019.05.003.
5. Ciofu O, Tolker-Nielsen T. 2019. Tolerance and resistance of *Pseudomonas aeruginosa* biofilms to antimicrobial agents—how *P aeruginosa* can escape antibiotics. Front Microbiol 10:913. https://doi.org/10.3389/fmicb.2019.00913.
6. Nickel JC, Wright JB, Ruseska I, Marrie TJ, Whitfield C, Costerton JW. 1985. Antibiotic resistance of *Pseudomonas aeruginosa* colonizing a urinary catheter in vitro. Eur J Clin Microbiol 4:213–218. https://doi.org/10.1007/BF02013600.
7. Walters MC, III, Roe F, Bugnicourt A, Franklin MJ, Stewart PS. 2003. Contributions of antibiotic penetration, oxygen limitation, and low metabolic activity to tolerance of *Pseudomonas aeruginosa* biofilms to ciprofloxacin and tobramycin. Antimicrob Agents Chemother 47:317–323. https://doi.org/10.1128/AAC.47.1.317-323.2003.
8. Borriello G, Werner E, Roe F, Kim AM, Ehrlich GD, Stewart PS. 2004. Oxygen limitation contributes to antibiotic tolerance of *Pseudomonas aeruginosa* in biofilms. Antimicrob Agents Chemother 48:2659–2664. https://doi.org/10.1128/AAC.48.7.2659-2664.2004.
9. Field TR, White A, Elborn JS, Tunney MM. 2005. Effect of oxygen limitation on the in vitro antimicrobial susceptibility of clinical isolates of *Pseudomonas aeruginosa* grown planktonically and as biofilms. Eur J Clin Microbiol Infect Dis 24:677–687. https://doi.org/10.1007/s10096-005-0031-9.
10. Hill D, Rose B, Pajkos A, Robinson M, Bye P, Bell S, Elkins M, Thompson B, Macleod C, Aaron SD, Harbour C. 2005. Antibiotic susceptibilities of *Pseudomonas aeruginosa* isolates derived from patients with cystic fibrosis under aerobic, anaerobic, and biofilm conditions. J Clin Microbiol 43: 5085–5090. https://doi.org/10.1128/JCM.43.10.5085-5090.2005.
11. Pamp SJ, Gjermansen M, Johansen HK, Tolker-Nielsen T. 2008. Tolerance to the antimicrobial peptide colistin in *Pseudomonas aeruginosa* biofilms is linked to metabolically active cells, and depends on the pmr and mexAB-oprM genes. Mol Microbiol 68:223–240. https://doi.org/10.1111/j.1365-2958.2008.06152.x.
12. Zhang L, Mah T-F. 2008. Involvement of a novel efflux system in biofilm specific resistance to antibiotics. J Bacteriol 190:4447–4452. https://doi.org/10.1128/JB.01655-07.
13. Folsom JP, Richards L, Pitts B, Roe F, Ehrlich GD, Parker A, Mazurie A, Stewart PS. 2010. Physiology of *Pseudomonas aeruginosa* in biofilms as revealed by transcriptome analysis. BMC Microbiol 10:294. https://doi.org/10.1186/1471-2180-10-294.
14. Nguyen D, Joshi-Datar A, Lepine F, Bauerle E, Olakanmi O, Beer K, McKay G, Siehnel R, Schafhauser J, Wang Y, Britigan BE, Singh PK. 2011. Active starvation responses mediate antibiotic tolerance in biofilms and nutrient-limited bacteria. Science 334:982–986. https://doi.org/10.1126/science.1211037.
15. Liao J, Sauer K. 2012. The MerR-like transcriptional regulator BrlR contributes to *Pseudomonas aeruginosa* biofilm tolerance. J Bacteriol 194:4823–4836. https://doi.org/10.1128/JB.00765-12.
16. Williamson KS, Richards LA, Perez-Osorio AC, Pitts B, McInnerney K, Stewart PS, Franklin MJ. 2012. Heterogeneity in *Pseudomonas aeruginosa* biofilms includes expression of ribosome hibernation factors in the antibiotic-tolerant subpopulation and hypoxia-induced stress response in the metabolically active population. J Bacteriol 194:2062–2073. https://doi.org/10.1128/JB.00022-12.
17. Zhang L, Chiang W-C, Gao Q, Givskov M, Tolker-Nielsen T, Yang L, Zhang G. 2012. The catabolite repression control protein Crc plays a role in the development of antimicrobial-tolerant subpopulations in *Pseudomonas aeruginosa* biofilms. Microbiology (Reading) 158:3014–3019. https://doi.org/10.1099/mic.0.061192-0.
18. Gupta K, Marques CN, Petrova OE, Sauer K. 2013. Antimicrobial tolerance of *Pseudomonas aeruginosa* biofilms is activated during an early developmental stage and requires the two-component hybrid SagS. J Bacteriol 195:4975–4987. https://doi.org/10.1128/JB.00732-13.
19. Liao J, Schurr MJ, Sauer K. 2013. The MerR-like regulator BrlR confers biofilm tolerance by activating multidrug-efflux pumps in *Pseudomonas aeruginosa* biofilms. J Bacteriol 195:3352–3363. https://doi.org/10.1128/JB.00318-13.
20. Stewart PS, Franklin MJ, Williamson KS, Folsom JP, Boegli L, James GA. 2015. Contribution of stress responses to antibiotic tolerance in *Pseudomonas aeruginosa* biofilms. Antimicrob Agents Chemother 59:3838–3847. https://doi.org/10.1128/AAC.00433-15.
21. Poudyal B, Sauer K. 2018. The ABC of biofilm drug tolerance: the MerR-like regulator BrlR is an activator of ABC transport systems, with PA1874-77 contributing to the tolerance of *Pseudomonas aeruginosa* biofilms to tobramycin. Antimicrob Agents Chemother 62:e01981-17. https://doi.org/10.1128/AAC.01981-17.
22. Poudyal B, Sauer K. 2018. PA3177 encodes an active diguanylate cyclase that contributes to the biofilm antimicrobial tolerance but not biofilm formation by *P. aeruginosa*. Antimicrob Agents Chemother 62:e01049-18. https://doi.org/10.1128/AAC.01049-18.
23. Marques CNH, Nelson SM. 2019. Pharmacodynamics of ciprofloxacin against *Pseudomonas aeruginosa* planktonic and biofilm-derived cells. Lett Appl Microbiol 68:350–359. https://doi.org/10.1111/lam.13126.
24. Schiessl KT, Hu F, Jo J, Nazia SZ, Wang B, Price-Whelan A, Min W, Dietrich LEP. 2019. Phenazine production promotes antibiotic tolerance and metabolic heterogeneity in *Pseudomonas aeruginosa* biofilms. Nat Commun 10:762. https://doi.org/10.1038/s41467-019-08733-w.
25. Lozano C, López M, Rojo-Bezares B, Sáenz Y. 2020. Antimicrobial susceptibility testing in *Pseudomonas aeruginosa* biofilms: one step closer to a standardized method. Antibiotics (Basel) 9:880. https://doi.org/10.3390/antibiotics9120880.
26. Soares A, Alexandre K, Etienne M. 2020. Tolerance and persistence of *Pseudomonas aeruginosa* in biofilms exposed to antibiotics: molecular mechanisms, antibiotic strategies and therapeutic perspectives. Front Microbiol 11:2057. https://doi.org/10.3389/fmicb.2020.02057.
27. Wannigama DL, Hurst C, Hongsing P, Pearson L, Saethang T, Chantaravisoot N, Singkham-In U, Luk-In S, Storer RJ, Chatsuwan T. 2020. A rapid and simple method for routine determination of antibiotic sensitivity to biofilm populations of *Pseudomonas aeruginosa*. Ann Clin Microbiol Antimicrob 19:8. https://doi.org/10.1186/s12941-020-00350-6.
28. Vidal R, Dominguez M, Urrutia H, Bello H, Garcia A, Gonzalez G, Zemelman R. 1997. Effect of imipenem and sulbactam on sessile cells of *Acinetobacter baumannii* growing in biofilm. Microbios 91:79–87.
29. Kim HA, Ryu SY, Seo I, Suh SI, Suh MH, Baek WK. 2015. Biofilm formation and colistin susceptibility of *Acinetobacter baumannii* isolated from Korean nosocomial samples. Microb Drug Resist 21:452–457. https://doi.org/10.1089/mdr.2014.0236.
30. Qi L, Li H, Zhang C, Liang B, Li J, Wang L, Du X, Liu X, Qiu S, Song H. 2016. Relationship between antibiotic resistance, biofilm formation, and biofilm-specific resistance in *Acinetobacter baumannii*. Front Microbiol 7: 483. https://doi.org/10.3389/fmicb.2016.00483.
31. Wang YC, Kuo SC, Yang YS, Lee YT, Chiu CH, Chuang MF, Lin JC, Chang FY, Chen TL. 2016. Individual or combined effects of meropenem, imipenem, sulbactam, colistin, and tigecycline on biofilm-embedded *Acinetobacter baumannii* and biofilm architecture. Antimicrob Agents Chemother 60:4670–4676. https://doi.org/10.1128/AAC.00551-16.

Downloaded from https://journals.asm.org/journal/aac on 19 April 2022 by 153.90.118.208.

32. Amin M, Navidifar T, Shooshtari FS, Rashno M, Savari M, Jahangirmehr F, Arshadi M. 2019. Association between biofilm formation, structure, and the expression levels of genes related to biofilm formation and biofilm-specific resistance of *Acinetobacter baumannii* strains isolated from burn infection in Ahvaz, Iran. Infect Drug Resist 12:3867–3881. https://doi.org/10.2147/IDR.S228981.
33. Da Cunda P, Iribarnegaray V, Papa-Ezdra R, Bado I, González MJ, Zunino P, Vignoli R, Scavone P. 2020. Characterization of the different stages of biofilm formation and antibiotic susceptibility in a clinical *Acinetobacter baumannii* strain. Microb Drug Resist 26:569–575. https://doi.org/10.1089/mdr.2019.0145.
34. Shenkutie AM, Yao MZ, Siu GK, Wong BKC, Leung PH. 2020. Biofilm-induced antibiotic resistance in clinical *Acinetobacter baumannii* isolates. Antibiotics (Basel) 9:817. https://doi.org/10.3390/antibiotics9110817.
35. Anwar H, Strap JL, Costerton JW. 1992. Kinetic interaction of biofilm cells of *Staphylococcus aureus* with cephalexin and tobramycin in a chemostat system. Antimicrob Agents Chemother 36:890–893. https://doi.org/10.1128/AAC.36.4.890.
36. Rose WE, Poppens PT. 2009. Impact of biofilm on the in vitro activity of vancomycin alone and in combination with tigecycline and rifampicin against *Staphylococcus aureus*. J Antimicrob Chemother 63:485–488. https://doi.org/10.1093/jac/dkn513.
37. Okuda K, Zendo T, Sugimoto S, Iwase T, Tajima A, Yamada S, Sonomoto K, Mizunoe Y. 2013. Effects of bacteriocins on methicillin-resistant *Staphylococcus aureus* biofilm. Antimicrob Agents Chemother 57:5572–5579. https://doi.org/10.1128/AAC.00888-13.
38. Pabst B, Pitts B, Lauchnor E, Stewart PS. 2016. Gel-entrapped *Staphylococcus aureus* bacteria as models of biofilm infection exhibit growth in dense aggregates, oxygen limitation, antibiotic tolerance, and heterogeneous gene expression. Antimicrob Agents Chemother 60:6294–6301. https://doi.org/10.1128/AAC.01336-16.
39. Ma D, Mandell JB, Donegan NP, Cheung AL, Ma W, Rothenberger S, Shanks RMQ, Richardson AR, Urish KL. 2019. The toxin-antitoxin MazEF drives *Staphylococcus aureus* biofilm formation, antibiotic tolerance, and chronic infection. mBio 10:e01658-19. https://doi.org/10.1128/mBio.01658-19.
40. Britt NS, Hazlett DS, Horvat RT, Liesman RM, Steed ME. 2020. Activity of pulmonary vancomycin exposures versus planktonic and biofilm isolates of methicillin-resistant *Staphylococcus aureus* from cystic fibrosis sputum. Int J Antimicrob Agents 55:105898. https://doi.org/10.1016/j.ijantimicag.2020.105898.
41. Meyer KJ, Taylor HB, Seidel J, Gates MF, Lewis K. 2020. Pulse dosing of antibiotic enhances killing of a *Staphylococcus aureus* biofilm. Front Microbiol 11:596227. https://doi.org/10.3389/fmicb.2020.596227.
42. Harrington NE, Sweeney E, Alav I, Allen F, Moat J, Harrison F. 2021. Antibiotic efficacy testing in an *ex vivo* model of *Pseudomonas aeruginosa* and *Staphylococcus aureus* biofilms in the cystic fibrosis lung. J Vis Exp 167:e62187. https://doi.org/10.3791/62187.
43. Kamble E, Pardesi K. 2021. Antibiotic tolerance in biofilm and stationary-phase planktonic cells of *Staphylococcus aureus*. Microb Drug Resist 27:3–12. https://doi.org/10.1089/mdr.2019.0425.
44. Moormeier DE, Endres JL, Mann EE, Sadykov MR, Horswill AR, Rice KC, Fey PD, Bayles KW. 2013. Use of microfluidic technology to analyze gene expression during *Staphylococcus aureus* biofilm formation reveals distinct physiological niches. Appl Environ Microbiol 79:3413–3424. https://doi.org/10.1128/AEM.00395-13.
45. Dar D, Dar N, Cai L, Newman DK. 2021. Spatial transcriptomics of planktonic and sessile bacterial populations at single-cell resolution. Science 373:eabi4882. https://doi.org/10.1126/science.abi4882.
46. Emms DM, Kelly S. 2015. OrthoFinder: solving fundamental biases in whole genome comparisons dramatically improves orthogroup inference accuracy. Genome Biol 16:157. https://doi.org/10.1186/s13059-015-0721-2.
47. Emms DM, Kelly S. 2019. OrthoFinder: phylogenetic orthology inference for comparative genomics. Genome Biol 20:238. https://doi.org/10.1186/s13059-019-1832-y.
48. Altenhoff A, Boeckmann B, Capella-Gutierrez S, Dalquen DA, DeLuca T, Forslund K, Huerta-Cepas J, Linard B, Pereira C, Pryszcz LP, Schreiber F, da Silva AS, Szklarczyk D, Train C-M, Bork P, Lecompte O, von Mering C, Xenarios I, Sjölander K, Jensen LJ, Martin MJ, Muffato M, Gabaldón T, Lewis SE, Thomas PD, Sonnhammer E, Dessimoz C, Quest for Orthologs Consortium. 2016. Standardized benchmarking in the quest for orthologs. Nat Methods 13:425–430. https://doi.org/10.1038/nmeth.3830.
49. Altenhoff AM, Garrayo-Ventas J, Cosentino S, Emms D, Glover NM, Hernández-Plaza A, Nevers Y, Sundesha V, Szklarczyk D, Fernández JM, Codó L, For Orthologs Consortium TQ, Gelpi JL, Huerta-Cepas J, Iwasaki W, Kelly S, Lecompte O, Muffato M, Martin MJ, Capella-Gutierrez S, Thomas PD, Sonnhammer E, Dessimoz C. 2020. The *Quest for Orthologs* benchmark service and consensus calls in 2020. Nucleic Acids Res 48:W538–W545. https://doi.org/10.1093/nar/gkaa308.
50. Xavier JC, Patil KR, Rocha I. 2018. Metabolic models and gene essentiality data reveal essential and conserved metabolism in prokaryotes. PLoS Comput Biol 14:e1006556. https://doi.org/10.1371/journal.pcbi.1006556.
51. Gallagher LA, Ramage E, Weiss EJ, Radey M, Hayden HS, Held KG, Huse HK, Zurawski DV, Brittnacher MJ, Colin M. 2015. Resources for genetic and genomic analysis of emerging pathogen *Acinetobacter baumannii*. J Bacteriol 197:2027–2035. https://doi.org/10.1128/JB.00131-15.
52. Stewart PS, White B, Boegli L, Hamerly T, Williamson KS, Franklin MJ, Bothner B, James GA, Fisher S, Vital-Lopez FG, Wallqvist A. 2019. Conceptual model of biofilm antibiotic tolerance that integrates phenomena of diffusion, metabolism, gene expression, and physiology. J Bacteriol 201:e00307-19. https://doi.org/10.1128/JB.00307-19.
53. Bernier SP, Lebeaux D, DeFrancesco AS, Valomon A, Soubigou G, Coppée JY, Ghigo JM, Beloin C. 2013. Starvation, together with the SOS response, mediates high biofilm-specific tolerance to the fluoroquinolone ofloxacin. PLoS Genet 9:e1003144. https://doi.org/10.1371/journal.pgen.1003144.
54. Stewart PS, Zhang T, Xu R, Pitts B, Walters MC, III, Roe F, Kikhney J, Moter A. 2016. Reaction-diffusion theory explains hypoxia and heterogeneous growth within microbial biofilms associated with chronic infections. NPJ Biofilms Microbiomes 2:16012. https://doi.org/10.1038/npjbiofilms.2016.12.
55. Wentland EJ, Stewart PS, Huang CT, McFeters GA. 1996. Spatial variations in growth rate within *Klebsiella pneumoniae* colonies and biofilm. Biotechnol Prog 12:316–321. https://doi.org/10.1021/bp9600243.
56. Kragh KN, Alhede M, Jensen PØ, Moser C, Scheike T, Jacobsen CS, Seier Poulsen S, Eickhardt-Sørensen SR, Trøstrup H, Christoffersen L, Hougen HP, Rickelt LF, Kühl M, Høiby N, Bjarnsholt T. 2014. Polymorphonuclear leukocytes restrict growth of *Pseudomonas aeruginosa* in the lungs of cystic fibrosis patients. Infect Immun 82:4477–4486. https://doi.org/10.1128/IAI.01969-14.
57. Werner E, Roe F, Bugnicourt A, Franklin MJ, Heydorn A, Molin S, Pitts B, Stewart PS. 2004. Stratified growth in *Pseudomonas aeruginosa* biofilms. Appl Environ Microbiol 70:6188–6196. https://doi.org/10.1128/AEM.70.10.6188-6196.2004.
58. Zheng Z, Stewart PS. 2004. Growth limitation of *Staphylococcus epidermidis* in biofilms contributes to rifampin tolerance. Biofilms 1:31–35. https://doi.org/10.1017/S1479050503001042.
59. Dal Co A, van Vliet S, Ackermann M. 2019. Emergent microscale gradients give rise to metabolic cross-feeding and antibiotic tolerance in clonal bacterial populations. Philos Trans R Soc Lond B Biol Sci 374:20190080. https://doi.org/10.1098/rstb.2019.0080.
60. Dötsch A, Eckweiler D, Schniederjans M, Zimmermann A, Jensen V, Scharfe M, Geffers R, Häussler S. 2012. The *Pseudomonas aeruginosa* transcriptome in planktonic cultures and static biofilms using RNA sequencing. PLoS One 7:e31092. https://doi.org/10.1371/journal.pone.0031092.
61. Alvarez-Ortega C, Harwood CS. 2007. Responses of *Pseudomonas aeruginosa* to low oxygen indicate that growth in the cystic fibrosis lung is by aerobic respiration. Mol Microbiol 65:153–165. https://doi.org/10.1111/j.1365-2958.2007.05772.x.
62. Lequette Y, Lee J-H, Ledgham F, Lazdunski A, Greenberg EP. 2006. A distinct QscR regulon in the *Pseudomonas aeruginosa* quorum-sensing circuit. J Bacteriol 188:3365–3370. https://doi.org/10.1128/JB.188.9.3365-3370.2006.
63. Nalca Y, Jänsch J, Bredenbruch F, Geffers F, Buer J, Häussler S. 2006. Quorum-sensing antagonistic activities of azithromycin in *Pseudomonas aeruginosa* PAO1: a global approach. Antimicrob Agents Chemother 50:1680–1688. https://doi.org/10.1128/AAC.50.5.1680-1688.2006.
64. Teitzel GM, Geddie A, De Long SK, Kirisits MJ, Whiteley M, Parsek MR. 2006. Survival and growth in the presence of elevated copper: transcriptional profiling of copper-stressed *Pseudomonas aeruginosa*. J Bacteriol 188:7242–7256. https://doi.org/10.1128/JB.00837-06.
65. Weiss A, Broach WH, Shaw LN. 2016. Characterizing the transcriptional adaptation of *Staphylococcus aureus* to stationary phase growth. Pathog Dis 74:ftw046. https://doi.org/10.1093/femspd/ftw046.
66. Jacobs AC, Sayood K, Olmsted SB, Blanchard CE, Hinrichs S, Russell D, Dunman PM. 2012. Characterization of the *Acinetobacter baumannii* growth phase-dependent and serum responsive transcriptomes. FEMS Immunol Med Microbiol 64:403–412. https://doi.org/10.1111/j.1574-695X.2011.00926.x.
67. Rumbo-Feal S, Gómez MJ, Gayoso C, Álvarez-Fraga L, Cabral MP, Aransay AM, Rodríguez-Ezpeleta N, Fullaondo A, Valle J, Tomás M, Bou G, Poza M. 2013. Whole transcriptome analysis of Acinetobacter baumannii assessed by RNA-sequencing reveals different mRNA expression profiles in biofilm compared

Downloaded from https://journals.asm.org/journal/aac on 19 April 2022 by 153.90.118.208.

to planktonic cells. PLoS One 8:e72968. https://doi.org/10.1371/journal.pone.0072968.
68. Bergkessel M, Delavaine L. 2021. Diversity in starvation survival strategies and outcomes among heterotrophic Proteobacteria. Microb Physiol 31:146–117. https://doi.org/10.1159/000516215.
69. Bhuiyan MS, Ellett F, Murray GL, Kostoulias X, Cerqueira GM, Schulze KE, Mahamad Maifiah MH, Li J, Creek DJ, Lieschke GJ, Peleg AY. 2016. *Acinetobacter baumannii* phenylacetic acid metabolism influences infection outcome through a direct effect on neutrophil chemotaxis. Proc Natl Acad Sci U S A 113:9599–9604. https://doi.org/10.1073/pnas.1523116113.
70. Xu Y, Maltesen RG, Larsen LH, Schønheyder HC, Le VQ, Nielsen JL, Nielsen PH, Thomsen TR, Nielsen KL. 2016. In vivo gene expression in a *Staphylococcus aureus* prosthetic joint infection characterized by RNA sequencing and metabolomics: a pilot study. BMC Microbiol 16:80. https://doi.org/10.1186/s12866-016-0695-6.
71. Tomlinson BR, Malof ME, Shaw LN. 2021. A global transcriptomic analysis of *Staphylococcus aureus* biofilm formation across diverse clonal lineages. Microb Genom 7:e000598. https://doi.org/10.1099/mgen.0.000598.
72. Resch A, Rosenstein R, Nerz C, Götz F. 2005. Differential gene expression profiling of *Staphylococcus aureus* cultivated under biofilm and planktonic conditions. Appl Environ Microbiol 71:2663–2676. https://doi.org/10.1128/AEM.71.5.2663-2676.2005.
73. Yao Y, Sturdevant DE, Otto M. 2005. Genomewide analysis of gene expression in *Staphylococcus epidermidis* biofilms: insights into the pathophysiology of *S. epidermidis* biofilms and the role of phenol-soluble modulins in formation of biofilms. J Infect Dis 191:289–298. https://doi.org/10.1086/426945.
74. Beenken KE, Dunman PM, McAleese F, Macapagal D, Murphy E, Projan SJ, Blevins JS, Smeltzer MS. 2004. Global gene expression in *Staphylococcus aureus* biofilms. J Bacteriol 186:4665–4684. https://doi.org/10.1128/JB.186.14.4665-4684.2004.
75. Sønderholm M, Bjarnsholt T, Alhede M, Kolpen M, Jensen PØ, Kühl M, Kragh KN. 2017. The consequences of being in an infectious biofilm: microenvironmental conditions governing antibiotic tolerance. Int J Mol Sci 18:2688. https://doi.org/10.3390/ijms18122688.
76. Bjarnsholt T, Whiteley M, Rumbaugh KP, Stewart PS, Jensen PØ, Frimodt-Møller N. 2021. The importance of understanding the infectious microenvironment. Lancet Infect Dis. https://doi.org/10.1016/S1473-3099(21)00122-5.
77. Cirz RT, O'Neill BM, Hammond JA, Head SR, Romesberg FE. 2006. Defining the *Pseudomonas aeruginosa* SOS response and its role in the global response to the antibiotic ciprofloxacin. J Bacteriol 188:7101–7110. https://doi.org/10.1128/JB.00807-06.
78. Brazas MD, Breidenstein EB, Overhage J, Hancock RE. 2007. Role of *lon*, an ATP-dependent protease homolog, in resistance of *Pseudomonas aeruginosa* to ciprofloxacin. Antimicrob Agents Chemother 51:4276–4283. https://doi.org/10.1128/AAC.00830-07.
79. Breidenstein EB, Bains M, Hancock RE. 2012. Involvement of the *lon* protease in the SOS response triggered by ciprofloxacin in *Pseudomonas aeruginosa* PAO1. Antimicrob Agents Chemother 56:2879–2887. https://doi.org/10.1128/AAC.06014-11.
80. Muthaiyan A, Silverman JA, Jayaswal RK, Wilkinson BJ. 2008. Transcriptional profiling reveals that daptomycin induces the *Staphylococcus aureus* cell wall stress stimulon and genes responsive to membrane depolarization. Antimicrob Agents Chemother 52:980–990. https://doi.org/10.1128/AAC.01121-07.
81. Lechner S, Prax M, Lange B, Huber C, Eisenreich W, Herbig A, Nieselt K, Bertram R. 2014. Metabolic and transcriptional activities of *Staphylococcus aureus* challenged with high-doses of daptomycin. Int J Med Microbiol 304:931–940. https://doi.org/10.1016/j.ijmm.2014.05.008.
82. Hua X, Chen Q, Li X, Yu Y. 2014. Global transcriptional response of *Acinetobacter baumannii* to a subinhibitory concentration of tigecycline. Int J Antimicrob Agents 44:337–344. https://doi.org/10.1016/j.ijantimicag.2014.06.015.
83. Ma L, Wang J, Wang S, Anderson EM, Lam JS, Parsek MR, Wozniak DJ. 2012. Synthesis of multiple *Pseudomonas aeruginosa* biofilm matrix exopolysaccharides is post-transcriptionally regulated. Environ Microbiol 14: 1995–2005. https://doi.org/10.1111/j.1462-2920.2012.02753.x.
84. Romling U, Galperin MY, Gomelsky M. 2013. Cyclic di-GMP: the first 25 years of a universal bacterial second messenger. Microbiol Mol Biol Rev 77:1–52. https://doi.org/10.1128/MMBR.00043-12.
85. Merighi M, Lee VT, Hyodo M, Hayakawa Y, Lory S. 2007. The second messenger bis-(3′-5′)-cyclic-GMP and its PilZ domain-containing receptor Alg44 are required for alginate biosynthesis in *Pseudomonas aeruginosa*. Mol Microbiol 65:876–895. https://doi.org/10.1111/j.1365-2958.2007.05817.x.
86. Whitney JC, Whitfield GB, Marmont LS, Yip P, Neculai AM, Lobsanov YD, Robinson H, Ohman DE, Howell PL. 2015. Dimeric c-di-GMP is required for post-translational regulation of alginate production in *Pseudomonas aeruginosa*. J Biol Chem 290:12451–12462. https://doi.org/10.1074/jbc.M115.645051.
87. Franklin MJ, Nivens DE, Weadge JT, Howell PL. 2011. Biosynthesis of the *Pseudomonas aeruginosa* extracellular polysaccharides, alginate, Pel, and Psl. Front Microbiol 22:167. https://doi.org/10.3389/fmicb.2011.00167.
88. Chambers JR, Sauer K. 2013. The MerR-like regulator BrlR impairs *Pseudomonas aeruginosa* biofilm tolerance to colistin by repressing PhoPQ. J Bacteriol 195:4678–4688. https://doi.org/10.1128/JB.00834-13.
89. Petrova OE, Gupta K, Liao J, Goodwine JS, Sauer K. 2017. Divide and conquer: the *Pseudomonas aeruginosa* two-component hybrid SagS enables biofilm formation and recalcitrance of biofilm cells to antimicrobial agents via distinct regulatory circuits. Environ Microbiol 19:2005–2024. https://doi.org/10.1111/1462-2920.13719.
90. Lynch SV, Dixon L, Benoit MR, Brodie EL, Keyhan M, Hu P, Ackerley DF, Andersen GL, Matin A. 2007. Role of the *rapA* gene in controlling antibiotic resistance of *Escherichia coli* biofilms. Antimicrob Agents Chemother 51:3650–3658. https://doi.org/10.1128/AAC.00601-07.
91. Colvin KM, Gordon VD, Murakami K, Borlee BR, Wozniak DJ, Wong GCL, Parsek MR. 2011. The Pel polysaccharide can serve a structural and protective role in the biofilm matrix of *Pseudomonas aeruginosa*. PLoS Pathog 7:e10012164. https://doi.org/10.1371/journal.ppat.1001264.
92. Nilsson M, Jakobsen TH, Givskov M, Twetman S, Tolker-Nielsen T. 2019. Oxidative stress response plays a role in antibiotic tolerance of *Streptococcus mutans* biofilms. Microbiology (Reading) 165:334–342. https://doi.org/10.1099/mic.0.000773.
93. Billings N, Millan M, Caldara M, Rusconi R, Tarasova Y, Stocker R, Ribbeck K. 2013. The extracellular matrix component Psl provides fast-acting antibiotic defense in *Pseudomonas aeruginosa* biofilms. PLoS Pathog 9: e1003526. https://doi.org/10.1371/journal.ppat.1003526.
94. Hentzer M, Teitzel GM, Balzer GJ, Heydorn A, Molin S, Givskov M, Parsek MR. 2001. Alginate overproduction affects *Pseudomonas aeruginosa* biofilm structure and function. J Bacteriol 183:5395–5401. https://doi.org/10.1128/JB.183.18.5395-5401.2001.
95. Murakami K, Ono T, Viducic D, Somiya Y, Kariyama R, Hori K, Amoh T, Hirota K, Kumon H, Parsek MR, Miyake Y. 2017. Role of *psl* genes in antibiotic tolerance of adherent *Pseudomonas aeruginosa*. Antimicrob Agents Chemother 61:e02587-16. https://doi.org/10.1128/AAC.02587-16.
96. Goltermann L, Tolker-Nielsen T. 2017. Importance of the exopolysaccharide matrix in antimicrobial tolerance of *Pseudomonas aeruginosa* aggregates. Antimicrob Agents Chemother 61:e02696-16. https://doi.org/10.1128/AAC.02696-16.
97. Irie Y, Roberts AEL, Kragh KN, Gordon VD, Hutchison J, Allen RJ, Melaugh G, Bjarnsholt T, West SA, Diggle SP. 2017. The *Pseudomonas aeruginosa* PSL polysaccharide is a social but noncheatable trait in biofilms. mBio 8: e00374-17. https://doi.org/10.1128/mBio.00374-17.
98. Yang L, Hu Y, Liu Y, Zhang J, Ulstrup J, Molin S. 2011. Distinct roles of extracellular polymeric substances in *Pseudomonas aeruginosa* biofilm development. Environ Microbiol 13:1705–1717. https://doi.org/10.1111/j.1462-2920.2011.02503.x.
99. Harrison JJ, Wade WD, Akierman S, Vacchi-Suzzi C, Stremick CA, Turner RJ, Ceri H. 2009. The chromosomal toxin gene *yafQ* is a determinant of multidrug tolerance for *Escherichia coli* growing in a biofilm. Antimicrob Agents Chemother 53:2253–2258. https://doi.org/10.1128/AAC.00043-09.
100. Honsa ES, Cooper VS, Mhaissen MN, Frank M, Shaker J, Iverson A, Rubnitz J, Hayden RT, Lee RE, Rock CO, Tuomanen EI, Wolf J, Rosch JW. 2017. RelA mutant *Enterococcus faecium* with multiantibiotic tolerance arising in an immunocompromised host. mBio 8:e02124-16. https://doi.org/10.1128/mBio.02124-16.
101. Salzer A, Keinhörster D, Kästle C, Kästle B, Wolz C. 2020. Small alarmone synthetases RelP and RelQ of *Staphylococcus aureus* are involved in biofilm formation and maintenance under cell wall stress conditions. Front Microbiol 11:575882. https://doi.org/10.3389/fmicb.2020.575882.
102. Stewart PS. 2003. Diffusion in biofilms. J Bacteriol 185:1485–1491. https://doi.org/10.1128/JB.185.5.1485-1491.2003.
103. Franklin MJ, Sandvik E, Yanardag S, Williamson KS. 2020. Functional characterization of the *Pseudomonas aeruginosa* ribosome hibernation-promoting factor. J Bacteriol 202:e00280-20. https://doi.org/10.1128/JB.00280-20.
104. Akiyama T, Williamson KS, Schaefer R, Pratt S, Chang CB, Franklin MJ. 2017. Resuscitation of *Pseudomonas aeruginosa* from dormancy requires hibernation promoting factor (PA4463) for ribosome preservation. Proc Natl Acad Sci U S A 114:3204–3209. https://doi.org/10.1073/pnas.1700695114.

Downloaded from https://journals.asm.org/journal/aac on 19 April 2022 by 153.90.118.208.

105. Song S, Wood TK. 2020. ppGpp ribosome dimerization model for bacterial persister formation and resuscitation. Biochem Biophys Res Commun 523:281–286. https://doi.org/10.1016/j.bbrc.2020.01.102.
106. Babin BM, Atangcho L, van Eldijk MB, Sweredoski MJ, Moradian A, Hess S, Tolker-Nielsen T, Newman DK, Tirrell DA. 2017. Selective proteomic analysis of antibiotic-tolerant cellular subpopulations in *Pseudomonas aeruginosa* biofilms. mBio 8:e01593-17. https://doi.org/10.1128/mBio.01593-17.
107. Sung K, Chon J, Kweon O, Nho S, Kim S, Park M, Paredes A, Lim JH, Khan SA, Phillips KS, Cerniglia CE. 2021. Dynamic adaptive response of *Pseudomonas aeruginosa* to clindamycin/rifampicin-impregnated catheters. Antibiotics 10:752. https://doi.org/10.3390/antibiotics10070752.
108. Stover CK, Pham XQ, Erwin AL, Mizoguchi SD, Warrener P, Hickey MJ, Brinkman FS, Hufnagle WO, Kowalik DJ, Lagrou M, Garber RL, Goltry L, Tolentino E, Westbrock-Wadman S, Yuan Y, Brody LL, Coulter SN, Folger KR, Kas A, Larbig K, Lim R, Smith K, Spencer D, Wong GK, Wu Z, Paulsen IT, Reizer J, Saier MH, Hancock RE, Lory S, Olson MV. 2000. Complete genome sequence of *Pseudomonas aeruginosa* PAO1, an opportunistic pathogen. Nature 406:959–964. https://doi.org/10.1038/35023079.
109. Kennedy AD, Otto M, Braughton KR, Whitney AR, Chen L, Mathema B, Mediavilla JR, Byrne KA, Parkins LD, Tenover FC, Kreiswirth BN, Musser JM, DeLeo FR. 2008. Epidemic community-associated methicillin-resistant *Staphylococcus aureus*: recent clonal expansion and diversification. Proc Natl Acad Sci U S A 105:1327–1332. https://doi.org/10.1073/pnas.0710217105.
110. Diep BA, Gill SR, Chang RF, Phan TH, Chen JH, Davidson MG, Lin F, Lin J, Carleton HA, Mongodin EF, Sensabaugh GF, Perdreau-Remington F. 2006. Complete genome sequence of USA300, an epidemic clone of community-acquired meticillin-resistant *Staphylococcus aureus*. Lancet 367:731–739. https://doi.org/10.1016/S0140-6736(06)68231-7.
111. Jacobs AC, Thompson MG, Black CC, Kessler JL, Clark LP, McQueary CN, Gancz HY, Corey BW, Moon JK, Si Y, Owen MT, Hallock JD, Kwak YI, Summers A, Li CZ, Rasko DA, Penwell WF, Honnold CL, Wise MC, Waterman PE, Lesho EP, Stewart RL, Actis LA, Palys TJ, Craft DW, Zurawski DV. 2014. AB5075, a highly virulent isolate of *Acinetobacter baumannii*, as a model strain for the evaluation of pathogenesis and antimicrobial treatments. mBio 5:e01076-14. https://doi.org/10.1128/mBio.01076-14.
112. Goeres DM, Hamilton MA, Beck NA, Buckingham-Meyer K, Hilyard JD, Loetterle LR, Lorenz LA, Walker DK, Stewart PS. 2009. A method for growing a biofilm under low shear at the air-liquid interface using the drip flow biofilm reactor. Nat Protoc 4:783–788. https://doi.org/10.1038/nprot.2009.59.
113. Ausubel FM, Brent R, Kingston RE. 1999. Short protocols in molecular biology, 4th ed. Wiley, New York, NY.
114. Dubois M, Gilles KA, Hamilton JK, Rebers PA, Smith F. 1956. Colorimetric method for determination of sugars and related substances. Anal Chem 28:350–356. https://doi.org/10.1021/ac60111a017.
115. Fuchs S, Mehlan H, Bernhardt J, Hennig A, Michalik S, Surmann K, Pané-Farré J, Giese A, Weiss S, Backert L, Herbig A, Nieselt K, Hecker M, Völker U, Mäder U. 2018. AureoWiki—the repository of the *Staphylococcus aureus* research and annotation community. Int J Med Microbiol 308:558–568. https://doi.org/10.1016/j.ijmm.2017.11.011.
116. Oliveros JC. 2007. Venny. An interactive tool for comparing lists with Venn's diagrams. https://bioinfogp.cnb.csic.es/tools/venny/index.html.

Downloaded from https://journals.asm.org/journal/aac on 19 April 2022 by 153.90.118.208.